

## Electronic Supplementary Information for *Journal of Material Chemistry C* manuscript:

### Photo-crosslinkable, deformable PMMA colloids

Matthias K. Klein,<sup>a</sup> Andreas Zumbusch\*<sup>a</sup> and Patrick Pfleiderer<sup>b</sup>

<sup>a</sup> *Department of Chemistry, University of Konstanz, 78457-Konstanz, Germany.  
Fax: +49 7531 88-3139; Tel: +49 7531 88-2357;  
E-mail: andreas.zumbusch@uni-konstanz.de*

<sup>b</sup> *Department of Physics, University of Konstanz, 78457-Konstanz, Germany.  
Fax: +49 (0) 7531 88-3090 ; Tel: +49 (0) 7531 88-2014;  
E-mail: patrick.pfleiderer@uni-konstanz.de*

#### 1. Synthesis of chemicals

##### 1.1 Synthesis of steric stabilizer PHSA-co-PMMA.

The steric stabilizer used for particle preparation was prepared according to the procedure reported by Ant et al.<sup>1</sup> First 47.9 g 12-hydroxystearic acid, 0.12 g methane sulfonic acid and 8.6 g toluene were refluxed at 175 °C for 18 hours to maintain the carboxyl terminated oligo(12-hydroxystearate) (OHSA). The azeotropic condensation was stopped when the theoretical amount of reaction water (2.3 ml) was collected. To functionalize the PHSA with a terminal methacrylate functionality, a mixture of 49.5 g PHSA-solution of the previous reaction, 46.7 g xylene, 0.054 g hydroquinone, 0.143 g N,N-dimethyldodecylamine (Armen DMCD) and 5.871 g glycidyl methacrylate (GM) were refluxed at 150 °C for 21 h. The final graft copolymer PHSA-co-PMMA was formed by continuously adding a mixture consisting of 49.2 g PHSA-GM, 22.44 g methyl methacrylate (MMA) and 2.50 g GM to a refluxing mixture of 17 g ethyl acetate (EA) and 8.5 g butyl acetate (BA) during 3 h. Refluxing was maintained for additional two hours during which two portions of 0.155 g azobisisobutyronitrile (AIBN) were added after 1 h each. Finally the mixture was diluted to a solid content of 40% by adding 16.15 g EA and 8.75 g BA.

## 1.2. Synthesis of 4-vinylbenzylalcohol.

4-vinylbenzylalcohol was synthesized according to Lee et al.<sup>2</sup> 1.6 ml of 4-vinylbenzylchlorid were reacted with 2.0 g sodium acetate in 5 ml dimethyl sulfoxid at 50 °C for 48 h. The aqueous phase was extracted 4 times with 25 ml ethyl acetate each and the reunified organic phases were dried over MgSO<sub>4</sub>. The crude 4-vinylbenzyl acetate was saponified with 0.6 g sodium hydroxide in a water/ethanol mixture (2.5 ml: 7.5 ml) at 100 °C during 3 h to the alcohol. The product was purified by column-chromatography (PE/EE= 4:1) to yield 4-vinylbenzylalcohol as slightly yellow oil. To prevent polymerization the product was stored at -18 °C in the dark.

## 1.3 Synthesis of rhodamine B 4-vinylbenzylester (RhB-V).

0.2 g Rhodamine B chloride were reacted with 0.160 g 4-vinylbenzylalcohol, 0.103 g N,N'-dicyclohexylcarbodiimide (DCC) and 0.005 g 4-(dimethylamino)pyridine (DMAP) in 5 ml dry dichloromethane under a nitrogen atmosphere according to Neises and Steglich.<sup>3</sup> The crude product was purified via column chromatography with CHCl<sub>3</sub>/methanol 9:1. After solvent evaporation the product was obtained as dark purple crystals with metallic gloss.

<sup>1</sup>H NMR (400 MHz, DMSO-*d*<sub>6</sub>, δ): 1.21 (t, *J* = 7 Hz, 12H, CH<sub>3</sub>), 3.64 (q, *J* = 7 Hz, 8H; CH<sub>2</sub>), 4.95 (s, 2H; CH<sub>2</sub>), 5.31 (t, *J* = 11 Hz, 1H; vinyl-H), 5.82 (t, *J* = 17.7 Hz, 1H; vinyl-H), 6.71 (dd, *J* = 17.7 Hz, 11.0 Hz, 1H; ArH), 6.83 (m, 2H, ArH), 6.9 (m, 2H, ArH), 6.96 (m, 2H, ArH), 7.04 (m, 2H, ArH), 7.27 (m, 2H, ArH), 7.48 (m, 1H, ArH), 7.82-7.92 (m, 2H, ArH), 8.27 (m, 1H; ArH); [*M*]<sup>+</sup> calcd for C<sub>37</sub>H<sub>39</sub>N<sub>2</sub>O<sub>3</sub><sup>+</sup>, 559.3; found, 559.4.

## 2. Particle preparation.

The different sized particle batches were prepared as described in the main text. The respective compositions of the polymerization mixtures are given in table 1. Before heating we added 0.057 g octyl mercaptane (OctSH) and 0.086 g AIBN to each polymerization mixture.

	CEA	MMA/MA-mixture [a]	RhB-V	dodecane/hexane-mixture [b]	stabilizer	mass fraction /%	Diameter / $\mu\text{m}$
LPX01	0.483	9.133	-	9.903	0.492	50.5	$1.15 \pm 0.04$
LPX02	0.472	8.851	-	9.241	0.478	51.47	$1.60 \pm 0.05$
LPX03	0.502	9.485	-	9.501	0.511	52.49	$1.81 \pm 0.07$
LPX04	0.476	8.857	0.0026	9.240	0.478	51.5	$1.40 \pm 0.04$
LPX05	0.471	8.85	-	9.217	0.487	51.53	$1.62 \pm 0.04$

[a] The ratio of the MMA/MA mixture is 98:2 (w/w); [b] The dodecane/hexane-ratio is 1:2 (w/w)

**Table S1.** Composition of initial polymerization mixtures of respective photo-crosslinkable latices LPX01, LPX02, LPX03, LPX04 and LPX05. Amounts are given in gram.

## 3. Extraction of particle diameters from SEM-Images.

In order to investigate the influence of the total mass content of the monomer mixture ~~over~~ on the final particle diameter, we varied the mass fraction of the monomer mixture ~~content~~, comprising MMA, MA, CEA and the stabilizer, between 50 to 52.5% (w/w) with respect to the total batch mass (Table S1). The mass fraction was already shown to have a crucial influence on the number of particles formed during nucleation due to enhanced solubility of the forming polymer chains at higher mass fractions of the monomer mixture leading to larger particles <sup>[2, 5]</sup>. The diameter of individual particles was extracted from Scanning Electron Microscopy (SEM) images sampling 100 particles for each particle batch. **Fig. S1E** shows that the final particle mean diameter can be simply predicted by adjusting the monomer mass

content. We prepared one additional particle batch denoted as LPX05 (black triangle in Fig. S1E). We selected a very similar mass fraction in comparison with LPX02 (51.53 % vs. 51.47 %) in order to demonstrate both the reliability and the precision of diameter control. The slight deviation of the mean diameter of LPX04 compared to LPX02 can be explained with the presence of the fluorescent comonomer RhB-V.

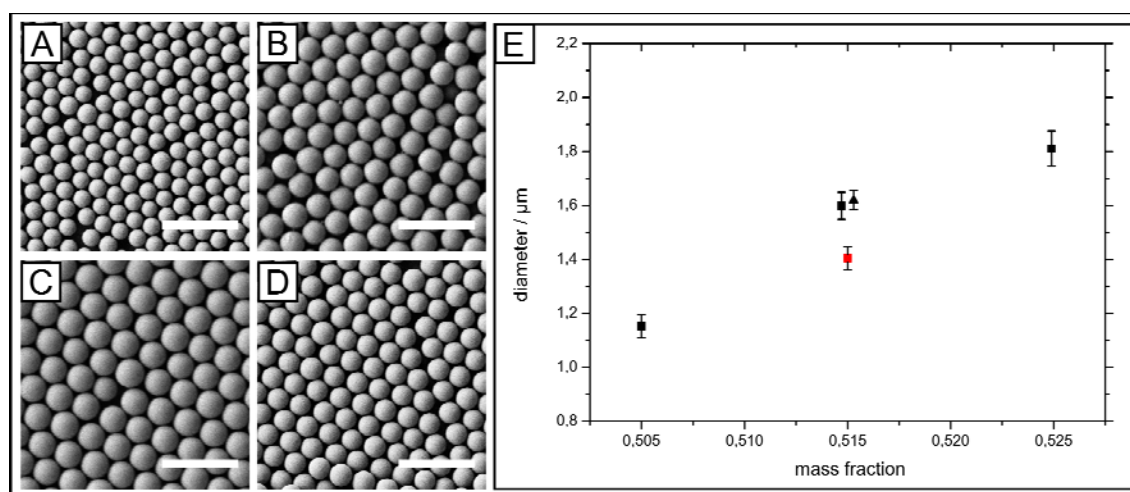


**Fig. S1** SEM-images of colloidal crystalline areas composed of LPX01 (A), LPX02 (B), LPX03 (C) and LPX04 (D) particles. E: Relation between mass fraction of initial polymerization mixture and final mean particle diameter with the corresponding standard deviation calculated from 100 particles for each particle batch. Black symbols represent non-fluorescent particle batches whereas the fluorescent batch is highlighted in red. The additional particle batch LPX05 is indicated by the black triangle. Scale bar: 5 μm.

## 4. Analytical data

### 4.1. Gel permeation chromatography of photo-crosslinkable particles.

The dried particles LPX02 were dissolved in THF at a concentration of 3 mg/ml. The resulting solution was passed through a 0.4  $\mu\text{m}$  PTFE-filter. The resulting size distributions recorded via UV detection at 280 nm and RI detection are shown in **Fig. S2**. The noisy structure in the case of UV detection was attributed to the antioxidant butyl hydroxyl toluene (BHT) in the THF used as eluent. BHT also shows a strong absorption in this region.

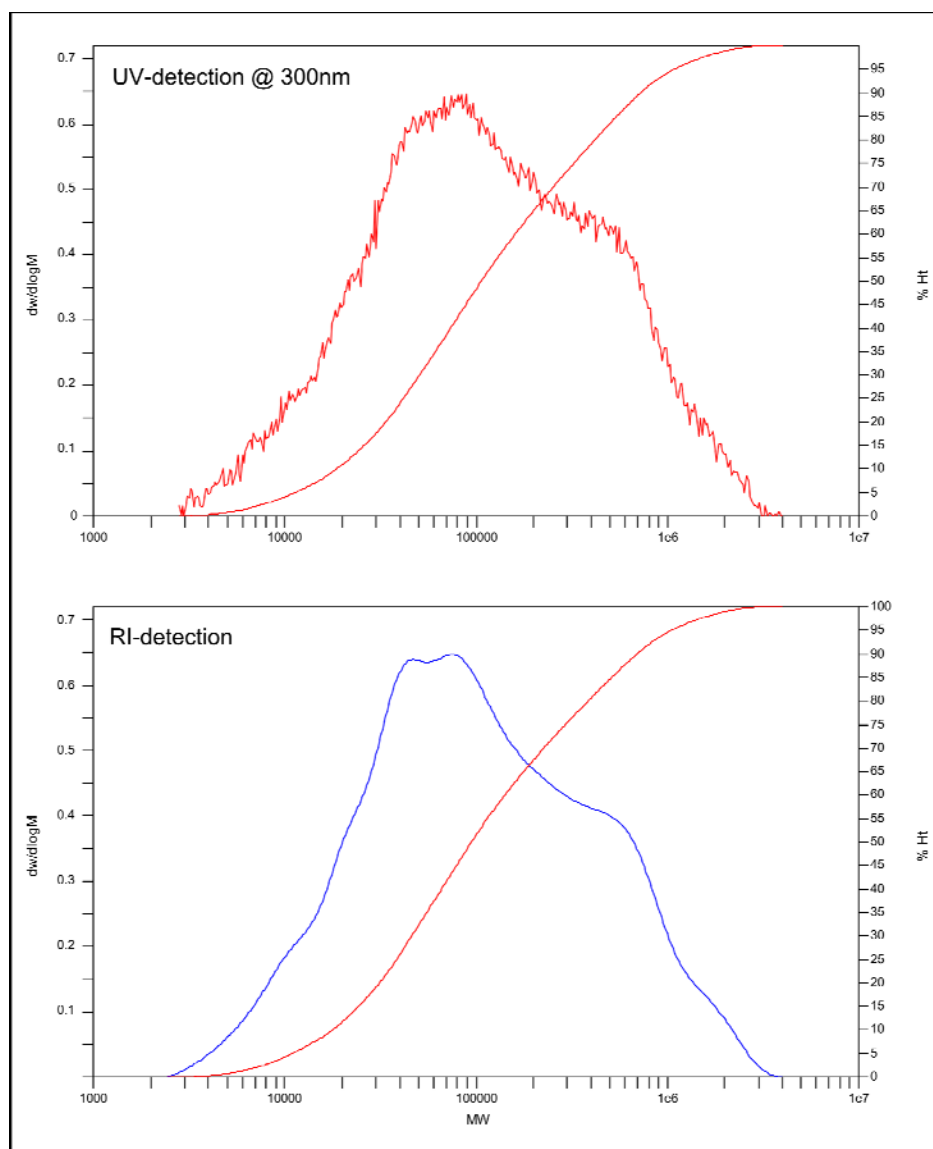


**Fig. S2** Gel permeation chromatograms of LPX02 dissolved in THF recorded under UV-detection (upper part) and by RI-detection (bottom part).

#### 4.2. $^1\text{H}$ -NMR spectroscopy of photo-crosslinkable copolymers.

The composition of the resulting photo-crosslinkable co polymer after particle preparation was analysed by  $^1\text{H}$ -NMR spectroscopy. The respective particle samples were dissolved in acetone- $\text{D}_6$  and  $^1\text{H}$ -NMR spectra comprising 128 scans each, were recorded. At low field, the spectra comprise the aromatic and vinylic resonances of the cinnamoyl residues between 7.9 ppm and 7.45 ppm followed by the resonance of the methoxy protons of the methyl methacrylate (MMA) repeat units at 3.63 ppm ending with the resonance of the randomly oriented methyl-groups of the polymer backbone ranging from 2.13 ppm to 0.67 ppm.

We compared the integrals of the 5 aromatic protons and the vicinal vinyl proton of the cinnamoyl residues between 8.02 ppm and 7.33 ppm to the integral of the methoxy-protons. An exemplary  $^1\text{H}$ -NMR-spectrum of the copolymer of the intermediate sized particles, denoted as LPX02, is depicted in **Fig. S3**. The resonances at 2.82 ppm and 2.05 ppm can be assigned to water and acetone- $\text{D}_6$  respectively. The analysis revealed the initial CEA/MMA ratio of  $\sim 2.7:100$  for each particle sample.

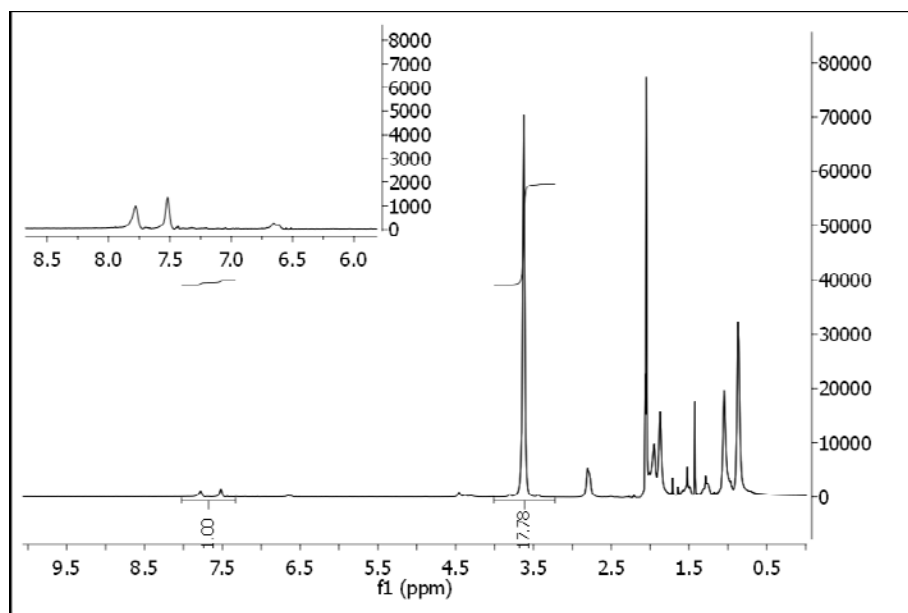


**Fig. S3**  $^1\text{H}$ -NMR spectrum of LPX02 dissolved in acetone- $\text{D}_6$  recorded at 400 MHz; 128 scans.

#### 4.3. Differential Scanning Calorimetry (DSC) of photo-crosslinkable precursor particles.

In order to determine the glass transition temperature of the photo-crosslinkable particles LPX02 we performed DSC-measurements on a DSC 204F1 (NETZSCH) (**Fig. S4**).

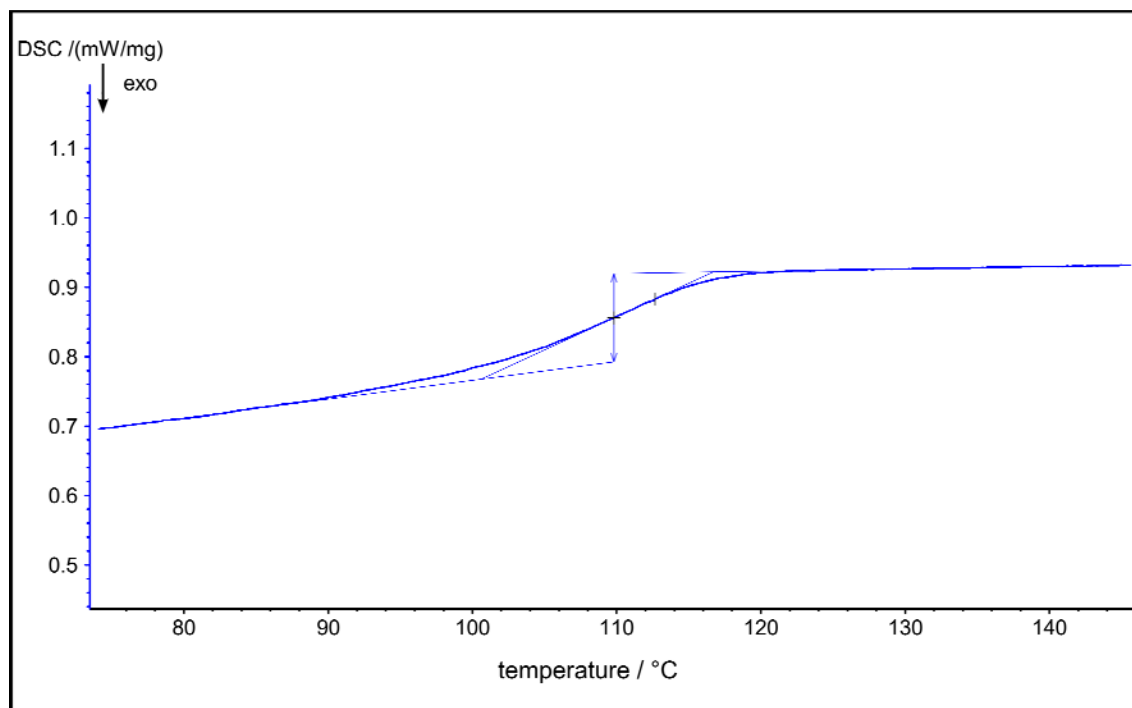


**Fig. S4** Differential Scanning Calorimetry (DSC) curve of the particle sample LPX02 used for stretching. (Heating rate 30 K/min).

#### 4.4. UV-VIS-spectroscopy on spin cast polymer films.

We prepared thin polymer films in order to follow the photo-dimerization process during particle illumination. After defined illumination times, the respective particle samples were thoroughly by repeated centrifugation and redispersion in petroleum ether (PE). Subsequently, the dried samples were dissolved in dichloromethane at concentrations of 45 mg/ml. At higher illumination times, we observed an increasing turbidity of the dichloromethane mixtures indicating an increase in gel content besides the dissolved polymer fraction. The resulting solutions/dispersions were spin cast at 4000 rpm on a quartz plate. After the immediate drying of the polymer films, the coated plates were placed in the beam path of the UV-VIS

spectrometer (Cary 50) and UV-VIS spectra were recorded (**Fig. S5**). As internal reference we selected the absorption band below 240 nm to follow the decrease of the cinnamoyl absorption band after subtracting the wavelength independent scattering background due to microgel formation. In the polymer films, which were prepared by dissolving the longest illuminated particle samples, we could even observe Bragg-diffraction which is caused by the formation of colloidal crystallites consisting of swollen microgel particles in the polymer films.

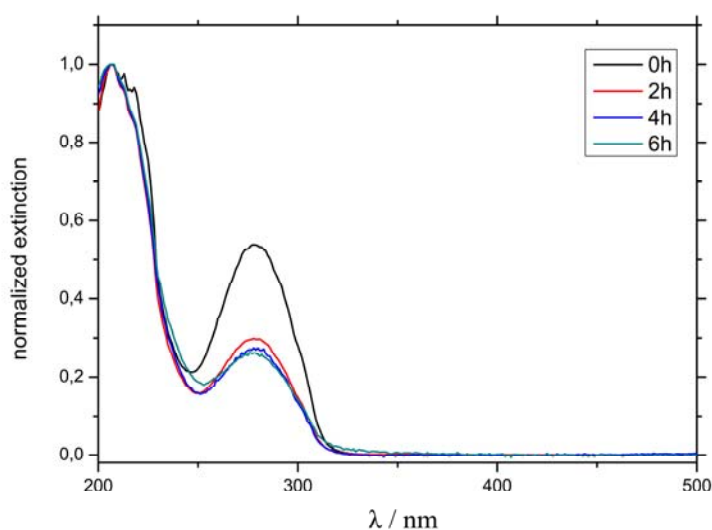


**Fig. S5** UV-VIS spectra on spin cast polymer films after different illumination times of the corresponding particle samples. Wavelength-independent scattering background has been subtracted.

#### 4.5. FT-IR spectroscopy of photo-crosslinkable particles.

As described in the main text we recorded FT-IR spectra on dried samples of the intermediate sized particles denoted as LPX02 and on the illuminated pendants. We compared the C=C stretching vibration located at  $1637\text{ cm}^{-1}$  with the C-CH<sub>3</sub> bending vibration at  $1388\text{ cm}^{-1}$  before and after illumination (**Fig. S6**). From this ratio we could estimate the relative fraction F of cinnmoyl residues which photo-dimerize and lead to photo-crosslinks according to the formula given in the main text.



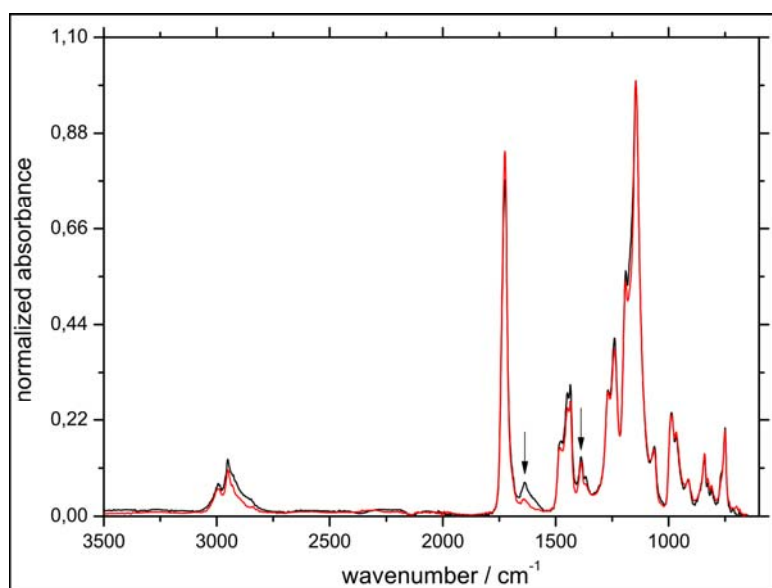


**Fig. S6** ATR FT-IR spectra of dried non-illuminated LPX02 particles (black line) and after 6 h of irradiation in dispersion (red line). The vinyl-stretching vibration of the cinnamoyl residues at  $1637\text{ cm}^{-1}$  and the C-CH<sub>3</sub> bending vibration at  $1388\text{ cm}^{-1}$  used as reference are highlighted with the black arrows.

#### 4.6. Determination of Gel-content of photo-crosslinkable particles.

Gel content was determined by the solvent extraction method. 35 mg of individual particle batches were dispersed in 2 ml decaline. After defined illumination times, the illuminated samples were centrifuged at 4000 rpm for 10 min and washed 4 times with petrolether. Subsequently the washed samples were dried in an oven for 2 h at 70 °C. The dried samples were weighed and then dispersed during 15 min in 3 ml THF and centrifuged at the previously defined settings. After centrifugation the supernatant was discarded and the residue was dispersed again in 3 ml THF. This procedure was repeated 5 times in total. After the last centrifugation step the solid residue was dried in the oven for 2 h at 100 °C and weighed again after cooling. The gel content was finally calculated by dividing the mass of the dried particle sample after solvent extraction  $m_{\text{ex}}$  by the mass before extraction  $m_0$  with THF.

## **5. Thermal and chemical stability**

### **5.1. Macroscale photolithography on particle layers.**

50  $\mu$ l of LPX01 particles, dispersed in hexane at a particle concentration of 3 mg/ml was dosed with a pipette and smoothly wiped over a microscopy coverslip followed by the immediate generation of partial two dimensional colloidal crystalline areas forced by dispersant evaporation. Subsequently the custom made paper mask, illustrated in **Fig. 5A** of the main text, was laid directly on the particle film. The assembly was illuminated with a 40 W UV-lamp (lamag) at 254 nm for 30 min. The lamp was placed at a distance of 3 cm above the mask. After illumination the paper mask was removed and the cover slip was three times intensely washed with 10 ml acetone to remove non-crosslinked areas. After complete drying the iridescent colours due to Bragg diffraction of the remaining illuminated areas appear.

### **5.2. Relaxation behaviour of the ellipsoids under locking conditions.**

As described in the main text, the illuminated and non-illuminated ellipsoids were subjected to the conditions selected to covalently lock the steric stabilizer on the particles surface. After addition of 10  $\mu$ l of the ring-opening catalyst Armen DMCD 70 mg of the respective ellipsoids dispersed in 5 ml decaline were heated to 130 °C and 200  $\mu$ l aliquots were taken after defined times. Changes in particle morphology can be roughly followed by optical microscopy. In order to quantify the relaxation behaviour in terms of changes in aspect ratio, average particle length and width, we recorded TEM-images to quantify those parameters. TEM-images were recorded on a Libra 120 instrument (acceleration voltage 120 kV). In total we investigated three samples comprising the particles right after the illumination procedure, the illuminated and non-illuminated particles after 8 h of heating in dispersion. For each

sample we analysed between 43 and 57 particles. The particles were detected and the above mentioned morphological parameters were analysed with the software iTEM Desktop.

### 5.3 Thermal stability of single ellipsoids.

The thermal stability of single illuminated and non illuminated ellipsoids was investigated by tempering the respective ellipsoids, distributed on cover slips at 200 °C for 1 h. The dispersions in decaline were spread over a coverslip and after evaporation of the decaline the samples were tempered at 200 °C. After cooling, the acquired DIC - micrographs depicted in **Fig. S7** revealed a significant difference in thermal stability as discussed in the main text.

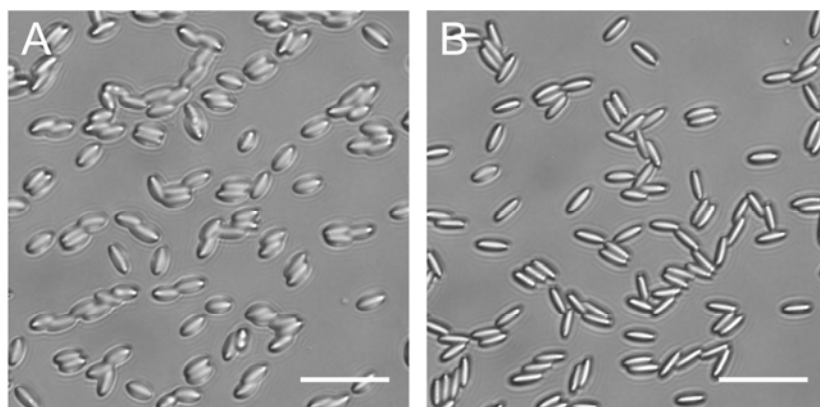


**Fig. S7** Optical microscopy images of non-illuminated (A) and illuminated (B) particles spread on microscopy cover slips after tempering at 200 °C for 1 hour. Scale bar: 10 μm.

### 6. Fluorophore loading of the microgel ellipsoids.

The photo-crosslinked ellipsoids can be subsequently loaded with the fluorescent dye Rhodamine B. 25 mg of the ellipsoids dispersed in 1 ml dodecane were mixed with 0.5 ml of a solution composed of 0.5 mg Rhodamine B dissolved in a cyclohexanone/acetone mixture (75:25(v/v)).<sup>4</sup> During stirring the colour changed from dark red to pink due to dye absorption of the particles. After 15 min the dispersion was centrifuged at 4000 rpm for 10 min and the

supernatant was discarded. The particles passed three centrifugation and washing cycles with 2 ml of decaline each.

### References:

1. L. Antl, J. W. Goodwin, R. D. Hill, R. H. Ottewill, S. M. Owens, S. Papworth and J. A. Waters, *Colloids Surf.*, 1986, **17**, 67-78.
2. E. Y. Lee, Y. Kim, J. S. Lee and J. Park, *Eur. J. Org. Chem.*, 2009, 2943-2946.
3. B. Neises and W. Steglich, *Angew. Chem.*, 1978, **17**.
4. A. D. Dinsmore, E. R. Weeks, V. Prasad, A. C. Levitt and D. A. Weitz, *Appl. Opt.*, 2001, **40**, 4152-4159.